



Evelyne Balteau¹, Tobias Leutritz², Nikolaus Weiskopf², Enrico Reimer², Antoine Lutti³, Martina F Callaghan⁴, Siawoosh Mohammadi⁵ and Karsten Tabelow⁶

¹Cyclotron Research Centre - GIGA-CRC in vivo imaging, University of Liege, Belgium, ²Department of Neurophysics, Max Planck Institute for Human Cognitive and Brain Sciences, Leipzig, Germany, ³Laboratoire de Recherche en Neuroimagerie, CHUV, University of Lausanne, Switzerland, ⁴Wellcome Trust Centre for Neuroimaging, University College London, United Kingdom, ⁵Institut für Systemische Neurowissenschaften, Universitätsklinikum Hamburg-Eppendorf, Germany, ⁶Weierstrass Institute for Applied Analysis and Stochastics, Berlin, Germany.

HIGHLIGHTS

PURPOSE: Quantitative magnetic resonance imaging (qMRI) helps reveal the biophysical properties governing MRI contrast. By eliminating instrumental biases and other contrast mechanisms influencing the signal amplitude, quantitative parameter maps can be derived and ultimately serve as *in vivo* biomarkers¹. **Biases in proton density (PD) map estimation** include radio-frequency transmit (B_1^+) and receive (B_1^-) fields and T_2^* weighting²⁻⁵. We focus on the T_2^* bias in multi-echo fast low angle shot (FLASH) protocols, where the T_2^* signal dependence is often neglected^{5,6}. Although often pointed out as a potential limitation especially in high iron content areas^{5,7,8}, the extent and severity of this bias and the evaluation of correction strategies have not yet been fully reported.

RESULTS: Simulated FLASH multiparameter mapping datasets with increasing noise levels were analysed with the hMRI toolbox and various processing strategies for PD estimation. Without T_2^* bias correction and with calibration to $PD=69\%$ in the WM, PD values were overestimated in the cortex (since $T_2^*_{GM} > T_2^*_{WM}$) and strongly underestimated in high iron content areas (globus pallidus, red nuclei, substantia nigra).

CONCLUSIONS: T_2^* bias correction is necessary to increase the sensitivity and specificity of qMRI in these areas. All methods taking T_2^* weighting bias into account are effective. However, method (2) shows lower SNR (relies on a single echo), while methods (1) (with T_2^* correction) and (3) perform similarly.

METHODS

SIMULATIONS: Multi-echo FLASH images (multiparameter mapping protocol⁷) with PD and T_1 -weighting (8 TE values equally spaced between 2.34 and 18.72ms, TR=25ms, FA=6° and 21° respectively) were simulated using the Ernst equation (assuming perfect RF spoiling⁹), SoS combination of the individual receiver coil signals and Gaussian noise added to the individual coil images (spatially variable SNR). R_2^* , R_1 , PD and B_1^+ maps generated using the hMRI toolbox¹⁰ (single subject dataset) were adaptively denoised^{11,12} and masked to serve as noise-free inputs to the simulation and as references to evaluate deviations of the PD and R_2^* map estimates. Synthetic coil sensitivities were generated using the Biot-Savart law^{13,14} for 48 coil elements distributed on a 24cm-diameter sphere (excluding neck aperture in the head coil).

PROCESSING: hMRI toolbox¹⁰ with ESTATICS model¹⁵ to estimate R_2^* maps and rational approximation of the Ernst equation⁶ to estimate R_1 and A (biased PD) maps. A maps accounted for B_1^+ bias only (based on the B_1^+ map input to data simulation). T_2^* correction factor² (optional), Unified Segmentation B_1^- bias correction^{7,16} and calibration ($PD_{WM} = 69\%$) were then applied to generate quantitative PD maps.

The A maps were derived either from:

- (1) the first 6 echoes of the PD-weighted images, averaged to increase SNR,
- (2) the first PD-weighted echo only (to reduce T_2^* bias),
- (3) extrapolation (TE=0) of the signal decay in the PDw images.

An optional T_2^* correction factor ($1/\text{mean}(\exp(-TE_i \cdot R_2^*))$) was applied voxel-wise to the A map before B_1^+ bias correction (ESTATICS-estimated R_2^* and mean calculated across TE_{1-6} (1) or TE_1 alone (2). No additional correction factor was required for (3). All the above methods are implemented in the hMRI toolbox¹⁰.

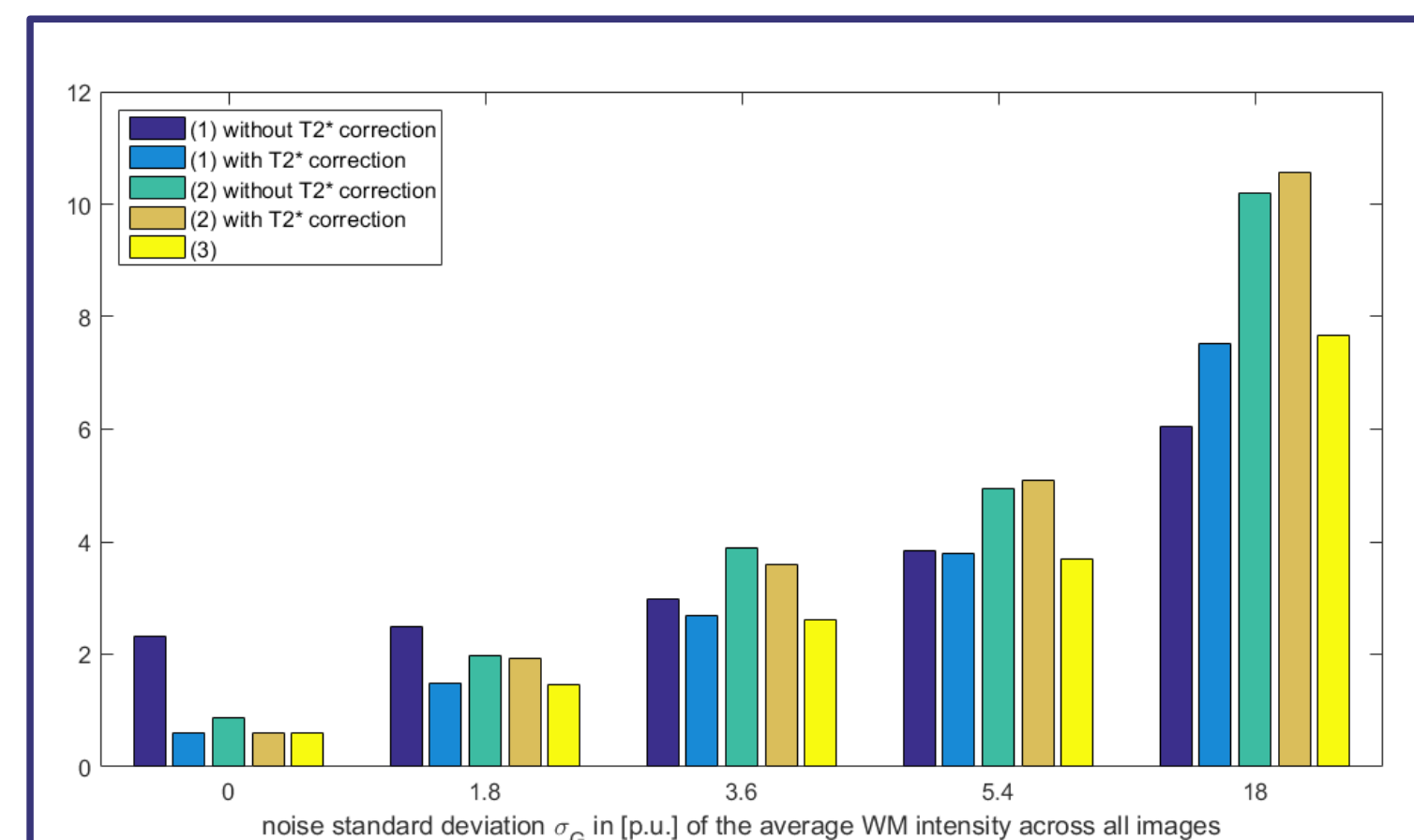


FIGURE 5 - Standard deviation of the PD error ($200 \cdot (PD - PD_{ref}) / (PD + PD_{ref})$) in p.u. in the WM for each method and increasing noise levels. Due to the calibration procedure, the average error in the WM is 0. With T_2^* correction, method (1) achieves better than method (2) due to the higher SNR of the input PD-weighted images (average over 6 echoes versus single echo). The T_2^* correction reduces the error in the PD estimate as long as the noise added by the R_2^* estimate is smaller than the variations due to T_2^* bias. TE=0 extrapolation (method (3)) performs similarly to method (1) with T_2^* correction.

REFERENCES

1. Weiskopf *et al.* *Curr Opin Neurol.* 2015;28(4):313-22. 2. Neeb *et al.* *Neuroimage.* 2006;31(3):1156-68. 3. Volz *et al.* *MRM* 2012;68(1):74-85. 4. Abbas *et al.* *MRM* 2014;72(6):1735-45. 5. Mezer *et al.* *HBM* 2016;37(10):3623-35. 6. Helms *et al.* *MRM* 2008;59(3):667-72. 7. Weiskopf *et al.* *Front Neurosci.* 2013;7:95. 8. Callaghan *et al.* *Neurobiol Aging.* 2014;35(8):1862-72. 9. Preibisch & Deichmann *MRM* 2009;61(1):125-35. 10. hMRI-Toolbox: <http://www.hmri.info> & Poster #2095. 11. Mohammadi *et al.* Preprint no. 2432, WIAS, Berlin, 2017, DOI 10.20347/WIAS.PREPRINT.2432. 12. Tabelow *et al.* *OHBM* 2016, Geneva. 13. Guerin-Kern *et al.* *IEEE Trans Med Imaging.* 2012;31(3), 626-636. 14. Matlab Framework for MRI Simulation and Reconstruction: http://bigwww.epfl.ch/algorithms/mri-reconstruction/code_v1-0.zip 15. Weiskopf *et al.* *Front Neurosci.* 2014;8:278. 16. Weiskopf *et al.* *Neuroimage.* 2011;54(3):2116-24. 17. Tofts PS, Quantitative MRI of the brain (chapter 4). John Wiley & Sons, Ltd, Chichester, UK. 18. Ellerbrock & Mohammadi *HBM* 2017, doi: 10.1002/hbm.23858. 19. Tabelow *et al.* *ISMRM* 2017, Honolulu.

ACKNOWLEDGEMENTS

EB received funding from the European Structural and Investment Fund / European Regional Development Fund & the Belgian Walloon Government, project BIOMED-HUB (programme 2014-2020). SM received funding from the European Union's Horizon 2020 research and innovation programme under the Marie Skłodowska-Curie grant agreement No 658589. NW and SM received funding from the BMBF (01EW1711A and B) in the framework of ERA-NET NEURON. The research leading to these results has also received funding from the European Research Council under the European Union's Seventh Framework Programme (FP7/2007-2013) / ERC grant agreement n° 616905. This project has received funding from the European Union's Horizon 2020 research and innovation programme under the grant agreement No 681094, and is supported by the Swiss State Secretariat for Education, Research and Innovation (SERI) under contract number 15.0137. MFC is supported by the MRC and Spinal Research Charity through the ERA-NET Neuron joint call (MR/R00050/1). The Wellcome Centre for Human Neuroimaging is supported by core funding from the Wellcome [203147/Z/16/Z].

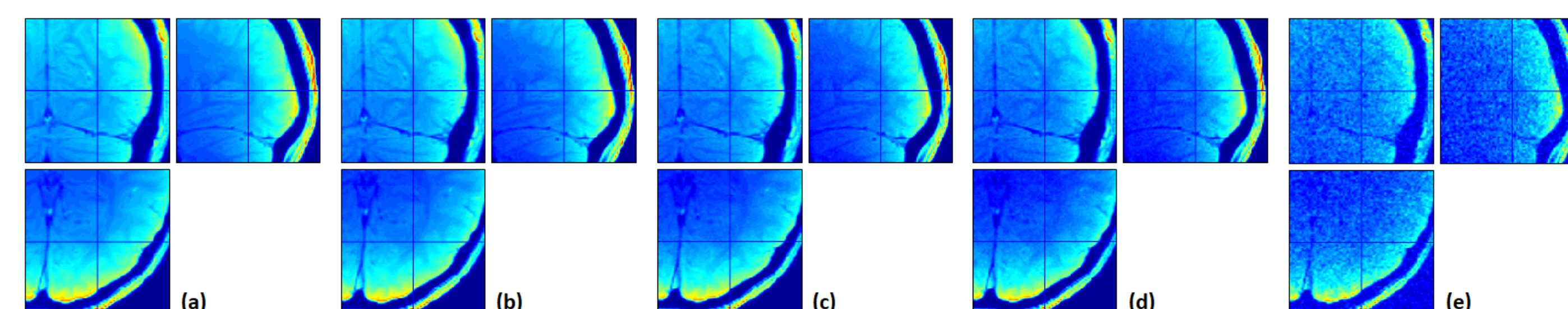


FIGURE 1 - Simulated PD-weighted images (TE=11.70ms) with increasing noise levels. (a) $\sigma_G = 0\%$, (b) $\sigma_G = 1.8\%$, (c) $\sigma_G = 3.6\%$, (d) $\sigma_G = 5.4\%$, (e) $\sigma_G = 18\%$. The standard deviation of the added Gaussian noise σ_G is expressed in p.u. (%) of the average signal measured in the white matter across all (PD-weighted and T_1 -weighted) simulated echoes.

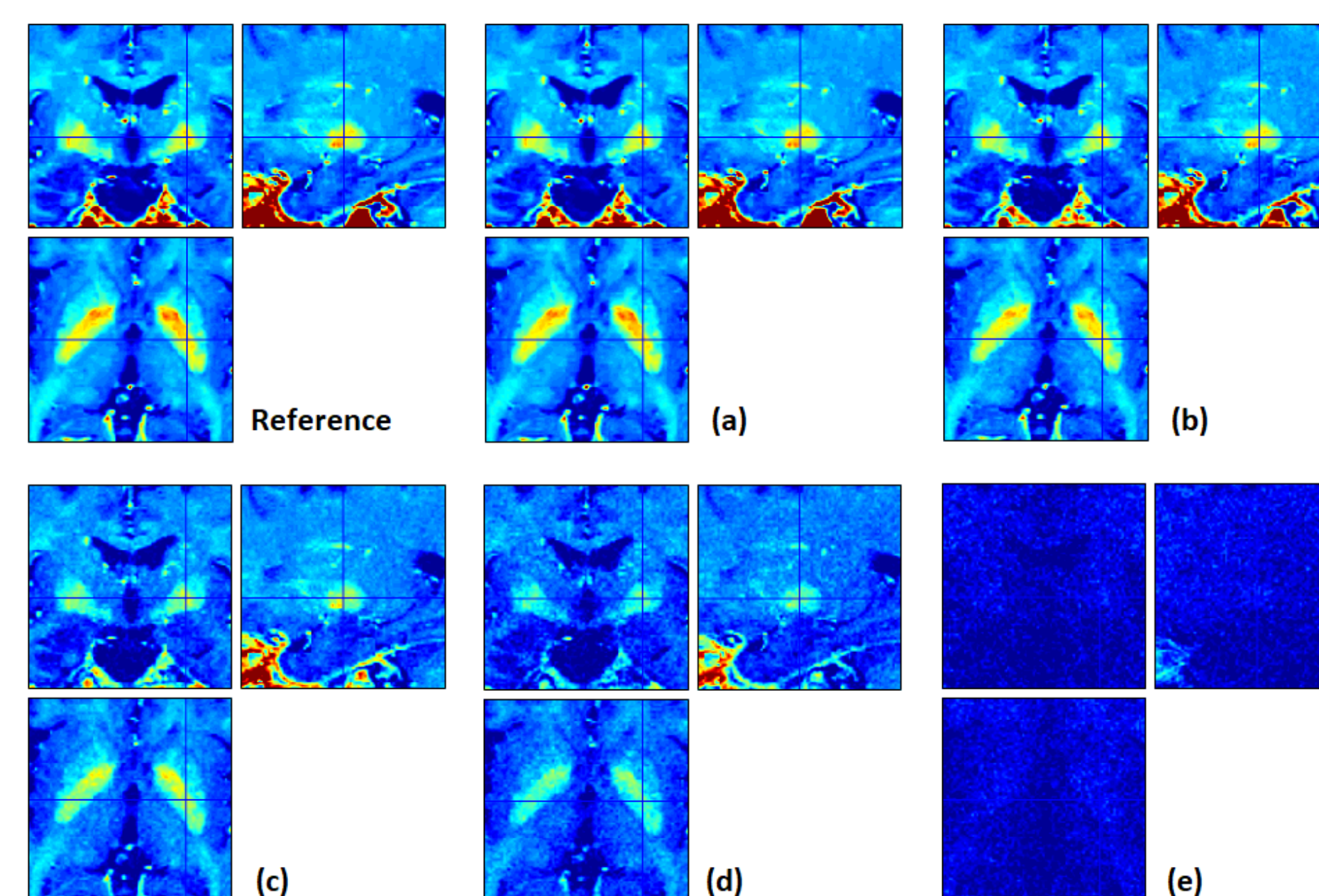
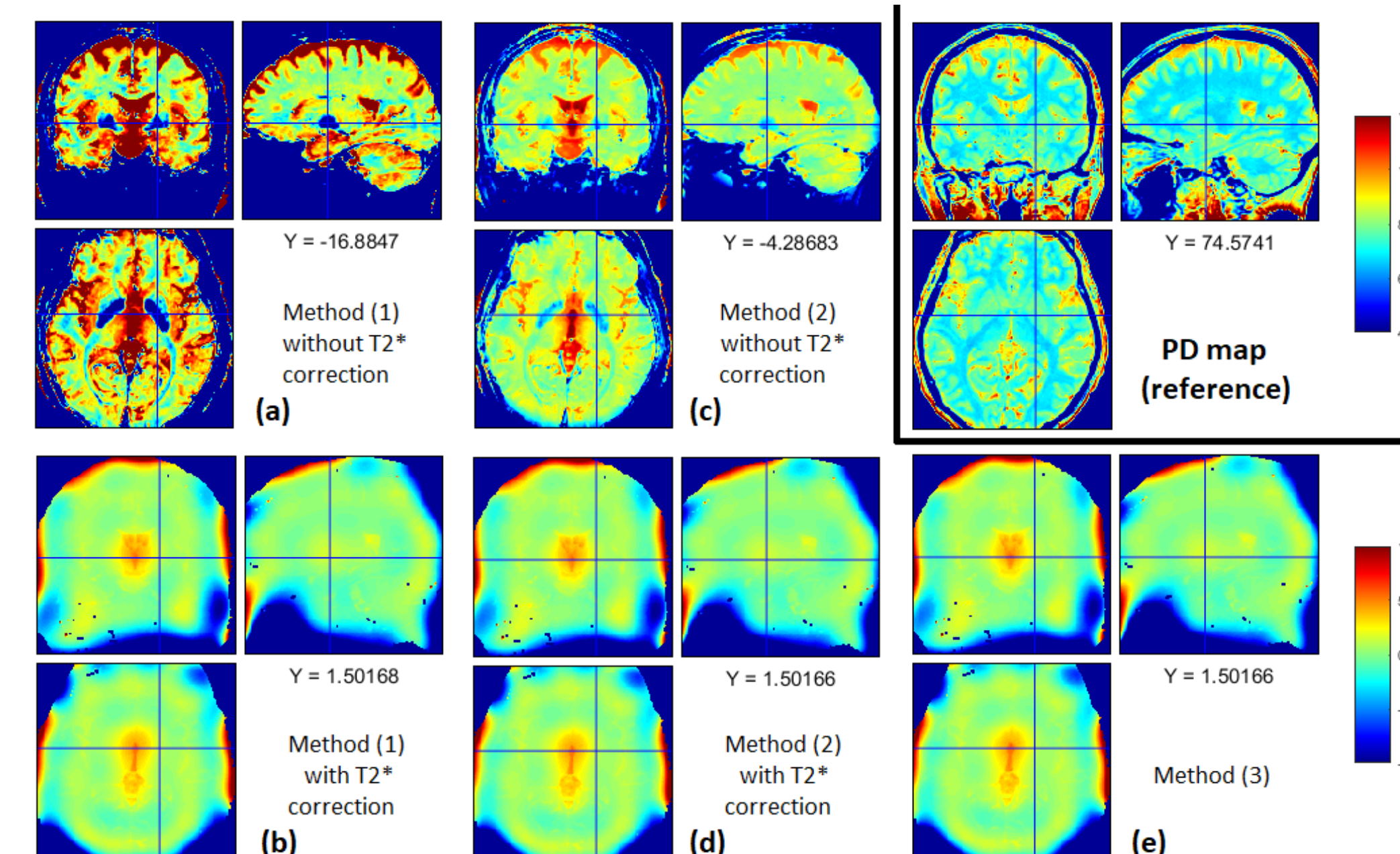


FIGURE 2 - R_2^* ESTATICS estimation. R_2^* reference image used for simulations and R_2^* ESTATICS estimates derived from images with increasing noise levels: (a) $\sigma_G = 0\%$, (b) $\sigma_G = 1.8\%$, (c) $\sigma_G = 3.6\%$, (d) $\sigma_G = 5.4\%$, (e) $\sigma_G = 18\%$. All maps are equally scaled between 0 and 70 s^{-1} . As expected, the increasing noise level leads to increasingly underestimated R_2^* values (noise floor effect due to the central chi-distributed noise in the SoS combined images)¹⁸.

FIGURE 3 - PD map estimation in the absence of noise. PD reference image (% water content) used for simulations (top right) and PD estimation error ($200 \cdot (PD_{est} - PD_{ref}) / (PD_{est} + PD_{ref})$) in p.u.) for each method (a-e). All methods taking the T_2^* weighting bias into account (b,d,e) provide good and almost identical results. Residual error is mostly related to the B bias field imperfect correction (smooth variation across the volume). Errors outlined by anatomical details are likely related to



the approximation of the Ernst equation used to estimate the quantitative maps⁵. Values (Y) within the globus pallidus (blue cross intersection) are reported under each sagittal view for comparison.

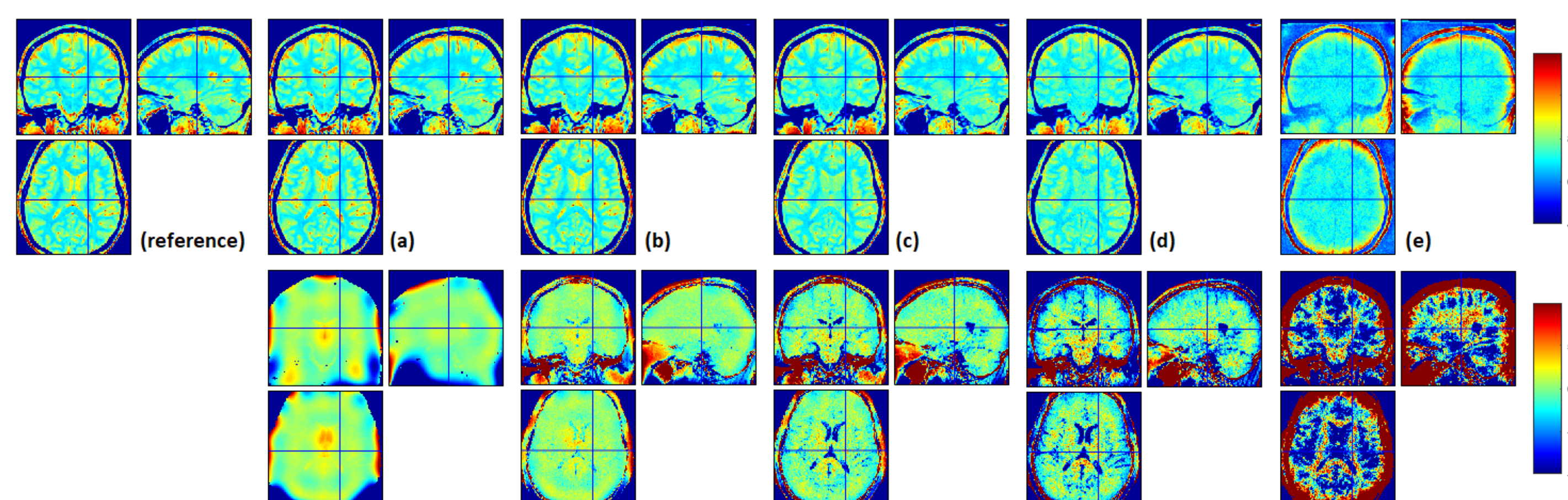


FIGURE 4 - PD map estimation in the presence of increasing noise levels. PD reference map, PD maps estimated with method (3) (top row) and corresponding PD error relative to the PD reference map (bottom row). Noise levels: (a) $\sigma_G = 0\%$, (b) $\sigma_G = 1.8\%$, (c) $\sigma_G = 3.6\%$, (d) $\sigma_G = 5.4\%$, (e) $\sigma_G = 18\%$. The results for methods (1) & (2) with T_2^* correction were very close to method (3) (data not shown), except for the lower SNR observed for method (2) (calculation relying on a single echo).